THE JOURNAL OF PHYSICAL CHEMISTRY C

Article

Cite This: J. Phys. Chem. C 2019, 123, 18315−18324

pubs.acs.org/JPCC

Monovalent and Divalent Cations at the α-Al_2O_3(0001)/Water Interface: How Cation Identity Affects Interfacial Ordering and Vibrational Dynamics

Published as part of The Journal of Physical Chemistry virtual special issue "Hai-Lung Dai Festschrift".

Stefan M. Piontek,[†] Aashish Tuladhar,[†,‡] Tim Marshall,[†] and Eric Borguet*[,†]

[†]Department of Chemistry, Temple University, 1901 N. 13th Street, Philadelphia, Pennsylvania 19122, United States

[‡]Physical Sciences Division, Physical and Computational Sciences Directorate, Pacific Northwest National Laboratory, Richland, Washington 99352, United States

Supporting Information

ABSTRACT: Mineral oxide/water interfaces are important for a wide range of industrial, geochemical, and biological processes. The reactivity of these interfaces is strongly impacted by the presence of ions. Thus, it is critical to understand how ions alter the interfacial environment. This can be achieved by measuring the changes in the structure and vibrational dynamics of interfacial water induced by the presence of ions in close vicinity to the mineral surface. The α-Al_2O_3(0001) surface represents a flexible platform to study the effect of ions on interfacial aqueous environments at positive, neutral, and negative surface charges. By using vibrational sum frequency generation (vSFG) in the frequency and time domains, we investigate how monovalent and divalent cations affect the hydrogen bonding environment of the first few layers of interfacial water next to α-Al_2O_3(0001). Our results indicate that monovalent cations, such as Li^+, Na^+, K^+, and Cs^+, appear to have lower binding affinities at the interface compared to Ca^{2+}, Sr^{2+}, and Ba^{2+}. This leads to an interfacial region that is structured in a cation valence dependent manner. The addition of divalent cations at the negatively charged interface (pH 10) increases the spectral intensity in the 3400 cm^{-1} region compared to neat pH 10 H_2O, in contrast to monovalent cations that only attenuate the vSFG signal. Time-resolved vSFG measurements reveal that the O−H vibrational lifetime (T_1) of interfacial species at pH 10 in the presence of NaCl and $BaCl_2$ remains similar. The restructuring of the interface seen in steady-state vSFG is manifested in the degree to which strongly hydrogen-bonded species recover to their original populations post excitation. By tracking the accumulation of ions at the interface via the vSFG response, we can characterize the unique surface arrangements of interfacial water molecules induced by monovalent and divalent cations at the α-Al_2O_3(0001)/water interface.

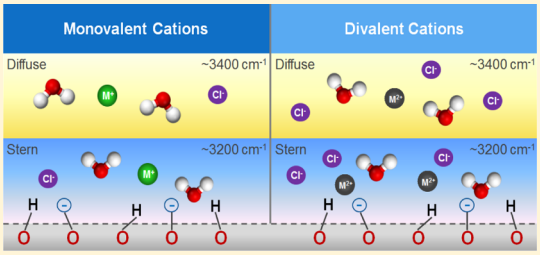

INTRODUCTION

Understanding water at solid/liquid interfaces is important because of its critical role in many chemical, biological, and environmental processes.[1] However, water rarely exists as a pure solvent and often solvates inorganic and organic ions, leading to changes in the macroscopic and microscopic properties of water. Extensive investigations of the effect of ions on the bulk water structure include ab initio calculations,[2] molecular dynamics simulations,[3−5] mid-IR pump−probe experiments,[6,7] static Raman measurements,[8] and X-ray absorption spectra.[9] However, bulk properties cannot be translated directly to infer the behavior of ions at interfaces. Therefore, techniques that inherently probe the interfacial region are required to understand the interplay between ions, water, and the surface.

Vibrational sum frequency generation (vSFG) spectroscopy, an inherently surface-specific technique, within the electric dipole approximation, allows us to probe molecular vibrations located exclusively at the solid/liquid interface.[10,11] To investigate the interfacial hydrogen bonding environment using vSFG, a narrowband visible pulse is combined with a broadband or tunable IR pulse resonant with the O−H stretching vibrations. This allows for surface-specific vibrational spectroscopy of water molecules and surface hydroxyls in the interfacial region.

Mineral oxide surfaces present an excellent opportunity to investigate ion effects on the structure and dynamics of interfacial water. Alumina, a geochemically abundant mineral oxide, is widely used in industrial catalysis, micro/nanoelectronics, ceramics, and filtration systems.[12−16] Alumina has a hexagonal crystal structure allowing for several low index surfaces (0001, $11\bar{2}0$, $1\bar{1}02$, and others) to be exposed.[17] The α-Al_2O_3(0001) face is terminated with a hydroxyl group density of ∼15 OH groups/nm^2[18−22] with one population

Received: February 19, 2019
Revised: May 13, 2019
Published: July 19, 2019

DOI: 10.1021/acs.jpcc.9b01618
J. Phys. Chem. C 2019, 123, 18315−18324

normal to the surface and the other in the plane of the surface.[23,24] Exposing other crystal planes allows for variation of the hydroxyl group density and aluminol group architecture. For example, the (0001) or *c* plane face contains Al_2O groups under vacuum while the $(11\bar{2}0)$ face, or *a* plane, possesses Al_2O, AlO, and Al_3O groups under vacuum.[17] Under ambient conditions, these groups are hydrogen terminated, resulting in an Al_2OH group for the *c* plane, and Al_2OH, $AlOH_2^{+0.5}$, $AlOH^{-0.5}$, and $Al_3OH^{+0.5}$ surface sites for the *a* plane.[25] These interfacial hydroxyl groups allow for pH-dependent modulation of the electrostatic potential at the α-Al_2O_3/water interface.[26]

The point of zero charge (PZC) for the (0001) face lies between pH 6−8 and this enables us to investigate the effect of ions at positive (<pH 6), neutral (pH 6−8), and negative (>pH 8) surfaces.[26,27] The PZC is not equivalent to the pK_a, and at pH 6, near the reported PZC of alumina, only a small fraction of surface OH groups will be charged from protonation or deprotonation events. Because surface charging of alumina should dictate the extent of ion adsorption, characterizing the interfacial structure as a function of bulk pH gives insight into how ionic contaminants could travel through ground water.[28]

Cations can modulate the complex behavior in biological systems such as ion channel gating and other processes, so understanding how they structure interfacial water populations in less-complicated environments may help our understanding of more complex phenomena.[29] The effect of cations on interfacial water structuring has been investigated by vSFG at the air/water,[30] the silica/water,[31,32] the TiO_2/water,[33] and the quartz/water[34] interfaces. Typically, the addition of cations at solid/liquid interfaces leads to attenuation of the vSFG response.[33,35] However, an increase in the amplitude of the vSFG response upon the addition of divalent cations (∼2 M) was reported at the hydrophobic air/vapor interface (pH 6).[30] Because the vSFG signal intensity is a measure of non-centrosymmetry, the authors argued that divalent cations order water more efficiently than the ion-free interface. Signal enhancement was the greatest for the weakly hydrogen-bonded species at ∼3400 cm^{-1}.[30] The vSFG measurements at the negatively charged silica/aqueous interface in the presence of monovalent and divalent cations showed that $MgCl_2$ attenuated the strongly hydrogen-bonded OH species arising from the water molecules closest to the interface while leaving the weakly hydrogen-bonded OH species unperturbed.[35] The authors hypothesized a "local hydrolysis model," where Mg^{2+} deprotonates surface silanols and forms ion-pairs with water adjacent to the surface after specific adsorption. This indicates that the effect of divalent cations on the local ordering of interfacial water is dependent on the type of the interface (hydrophobic vs hydrophilic). Monovalent and divalent cations induced valence-dependent ordering of interfacial water next to a negatively charged TiO_2/liquid interface, and it was concluded that divalent cations had a higher interfacial concentration than monovalent cations because of their increased ability to attenuate the spectral intensity in the OH stretch region.[33] The lower concentration of salts used (33 mM) could have contributed to the lack of enhancement for the 3400 cm^{-1} species, seen for ∼2 M cations at the hydrophobic air/vapor interface.[30] Clearly, divalent cations show unique behavior at mineral oxide/aqueous interfaces that is not well understood, especially their ability to selectively disrupt specific sub-populations of interfacial water species. Monovalent anions have shown a high degree of specificity in their ability to induce interfacial ordering and affect the vibrational dynamics of O−H species at the alumina/water interface.[36] The variety of cation induced organization of surface water molecules mentioned above motivates us to study how cations can impact interfacial species at the α-$Al_2O_3(0001)/H_2O$ interface as a function of ion coverage and surface charge.

While steady-state vSFG (SS-vSFG) is a powerful probe of the interfacial hydrogen bonding structure, time-resolved vSFG (TR-vSFG) measures the vibrational dynamics of excited O−H stretching modes, reflecting the local hydrogen bonding network strength.[37] We have previously investigated the strength of the interfacial hydrogen bonding network at the mineral oxide/water interface using time-resolved vSFG pump probe measurements.[36,38−42] Water O−H vibrational modes at the neutral (pH ≈ 2) SiO_2/H_2O interface relaxed to a hot vibrational ground state three times more slowly ($T_1 \approx 600$ fs) than species probed when the interface is negatively charged (pH ≈ 6−12), which displayed vibrational relaxation similar to bulk water ($T_1 \approx 200$ fs).[38] The positively and negatively charged α-$Al_2O_3(0001)$/water interfaces displayed faster vibrational dynamics (∼100 fs) than bulk water (∼200 fs), but bulk-like dynamics when uncharged.[38] The faster than bulk vibrational dynamics was attributed to an increase in the vibrational density of states in the ∼3000 cm^{-1} region, facilitated by strong alumina-water hydrogen bonding.[38] Only F^- affected vibrational dynamics at the α-$Al_2O_3(0001)$ interface compared to other halide anions (Cl^-, Br^-, and I^-).[36] Fluoride anions displayed specific adsorption at the interface, disrupting the interaction between the water and the alumina surface.[36,43] By investigating how cations perturb the interfacial hydrogen bonding network using SS-vSFG and TR-vSFG near a mineral oxide surface that can be positively and negatively charged via bulk pH modulation, we hope to further elucidate the complex behavior and interplay of ions in the interfacial region.

Our SS-vSFG and TR-vSFG results indicate that cations restructure water differently at positively, negatively, and uncharged α-$Al_2O_3(0001)/H_2O$ interfaces. Stronger adsorption of divalent cations in contrast to monovalent cations at the negatively charged alumina/water interface is revealed by the vSFG spectral intensity enhancement of the weakly hydrogen-bonded species at ∼3400 cm^{-1}. Concentration-dependent spectra in the 1×10^{-4} to 1 M range at pH 6 suggest that divalent cations have a stronger adsorption affinity for the interface compared to the monovalent cations. TR-vSFG measurements at the charged interfaces reveal that cation-induced interfacial structuring does not affect the lifetime of vibrational energy redistribution but can induce changes in relative populations of weakly and strongly hydrogen-bonded species post excitation. We show that cations not only restructure the α-$Al_2O_3(0001)/H_2O$ interfacial region, but do so in a cation identity dependent manner implicitly accounted for in the $\chi^{(2)}$ response, but not accounted for in the electrical double layer description of the interfacial potential[44] consistent with the recent results for the SiO_2/electrolyte interface.[45]

EXPERIMENTAL SECTION

Sample Preparation. α-$Al_2O_3(0001)$ cut equilateral roof prisms (15 × 13 × 13 × 15 mm) purchased from Team Photon Inc. (San Diego, CA) served as the alumina surface for our experiments. The prisms were first cleaned with the

DOI: 10.1021/acs.jpcc.9b01618
J. Phys. Chem. C 2019, 123, 18315−18324

"piranha" solution (1 volume concentrated H_2O_2: 3 volume concentrated H_2SO_4) for ~30 min in a walled Teflon dish. (**CAUTION:** *"piranha" is extremely reactive and can cause severe damage to skin/eyes. Handle using gloves, a face shield, a lab coat, and extreme care.*) To remove any remaining piranha solution, the prisms were then rinsed with copious amount of deionized water (>18.2 MΩ cm resistivity, Thermo Scientific Barnstead EASYpure II purification system with a UV lamp) and dried using ultrahigh pure N_2 gas. Lastly, the sample holder, a Teflon O-ring, and prisms are cleaned using low-pressure RF plasma for ~30 min (Harrick PDC-32G). Prisms are allowed to cool to room temp under vacuum and are exposed to Millipore water for ~15 min before experiments were performed. The prisms are mounted on a custom-fabricated sample holder.

Chemicals. Acidic and basic H_2O solutions were made using concentrated HCl (Sigma-Aldrich, TraceSELECT grade) and NaOH (Fluka Analytical, analytical grade), respectively. $BaCl_2$, $SrCl_2$, $CaCl_2$, KCl, and CsCl were purchased from Sigma-Aldrich at 99.99% purity by trace metal analysis while LiCl and NaCl, also 99.99% pure by trace metal analysis, were purchased from Alfa Aesar and Fluka Analytical, respectively.

Optical Setup. Approximately, 90% of a Ti:Sapphire regenerative amplifier laser system (Coherent, LIBRA—F-1K-110-HE+), operating at 1 kHz generating 5 mJ pulses at 800 nm with a pulse duration of 120 fs, pumps a commercial optical parametric amplifier (OPA) (Coherent, TOPAS-Prime HE). The remaining ~0.5 mJ of the Libra output passes through a narrow bandpass filter resulting in ~30 μJ pulses with ~2 nm of bandwidth (~30 cm^{-1}). An external difference frequency generation (DFG) $AgGaS_2$ (AgS) crystal attached to the output of the TOPAS generates tunable pulses in the mid-IR region (4000−1600 cm^{-1}). To record vSFG spectra over a region ~1000 cm^{-1} wide (defined by the 10% pedestal intensity level) in the OH stretch region, a broadband IR pulse profile is generated by employing a slight non-collinear DFG geometry with ~10 μJ/pulse centered at 3200−3400 cm^{-1}.[46] The incident angles were 60° (IR ≈ 5 μJ/pulse) and 54° (visible ≈ 30 μJ/pulse) for the steady-state vSFG measurements with a focused beam radius of ~75 and 200 μm, respectively. The incident angles were chosen to be slightly above the critical angle to ensure total internal reflection, which increases the magnitude of our collected vSFG signal. Reflected visible SFG photons were separated from scattered 800 nm photons with a 750 nm shortpass filter (Melles Griot) and sampled via a CCD detector (model Princeton Instruments) coupled to a spectrograph (300i Acton Research Corp.). Steady-state vSFG spectra were normalized via division of the nonresonant vSFG signal generated from a gold coated α-Al_2O_3(0001)prism (IR pulse profile) and corrected by a wavelength-dependent Fresnel factor to account for the dispersion of the refractive index in the OH stretch region. For time-resolved vSFG measurements, the IR beam is split with a ~3:1 ratio into a strong IR pump pulse used to remove population from the ground OH stretch vibrational state and a weaker IR + visible SFG probe that monitors population recovery while the pump−probe delay is scanned in time. The details for our pump−probe vSFG measurements have been described in detail previously.[38,39]

RESULTS AND DISCUSSION

Because vSFG is sensitive to the net orientation of interfacial water species, the effect of adding various ions can be observed via changes in the O−H stretch spectral features (Figure 1).

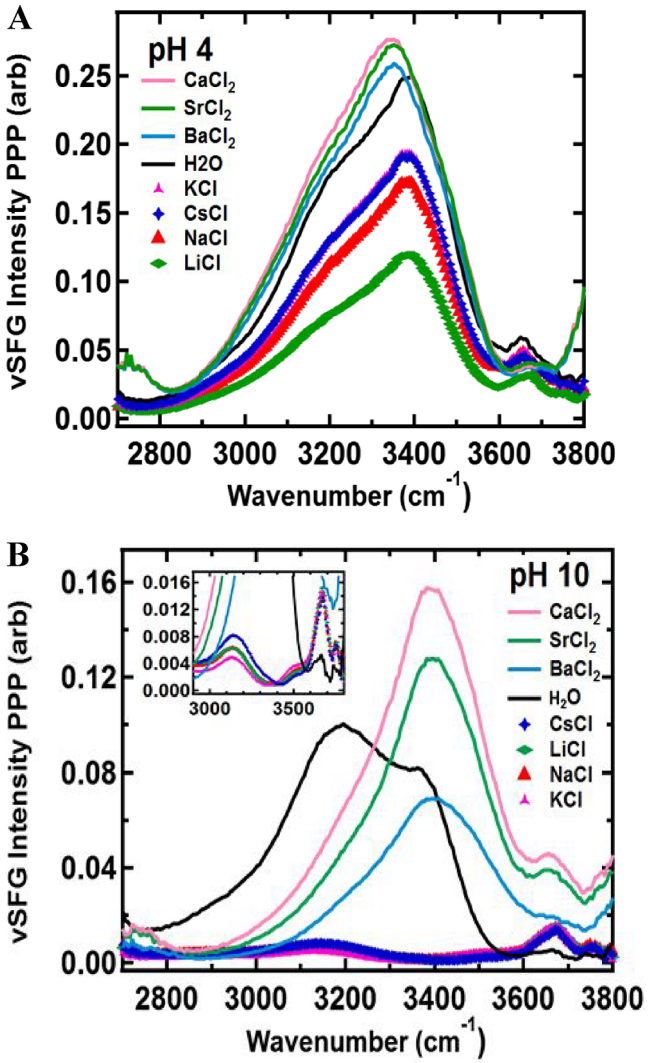

Figure 1. vSFG spectra of 0.1 M monovalent and divalent cation salts at (A) a positively (pH 4) and a (B) negatively (pH 10) charged α-Al_2O_3(0001)/H_2O interface. vSFG spectra have been normalized with respect to the shape of the infrared pulse profile and Fresnel factors. In panel (B), an inset shows the vSFG response of monovalent cations at the negatively charged interface.

Specifically, we focus on the weakly hydrogen-bonded water molecules at ~3400 cm^{-1} and the strongly hydrogen-bonded water at ~3200 cm^{-1}.[26,27,38] It should be noted that these peak assignments are still somewhat controversial because of the coupling between OH stretches and the overtone of the bend (Fermi resonance) observed at the liquid/vapor[47] and silica/water interfaces.[48,49] Free OH species thought to originate from non-hydrogen-bonded aluminols and water molecules have also been observed in the ~3700 cm^{-1} region.[27,40,50] If ions approach the interfacial region, surface water molecules can reorient themselves to solvate these ions and minimize the free energy of the interface. These changes in the surface water orientation can then be tracked via the vSFG response in the OH stretching region, giving insight into the structure of the first few layers of water at the interface.

Cations can reorganize the solvent and/or selectively adsorb at a variety of solid/water and air/water interfaces.[31,33,51] To investigate cation effects at the charged α-Al_2O_3(0001)/water interface, vSFG spectra were recorded for 0.1 M solutions of

DOI: 10.1021/acs.jpcc.9b01618
J. Phys. Chem. C 2019, 123, 18315−18324

monovalent and divalent cations at pH = 4 and pH = 10 with the PPP polarization combination (Figure 1) where the polarization of the SFG, visible, and IR photons is listed in order of decreasing photon energy. Our angles of incidence were carefully chosen to ensure that primarily χ_{zzz} is sampled for the PPP experimental geometry (Figure S5). Monovalent and divalent species at the positively charged interface induce qualitatively similar spectral profiles (Figure S1), but monovalent cations attenuate the vSFG spectral intensity while divalent cations slightly increase the vSFG response compared to pH 4 H_2O. For monovalent cations, both Cs^+ and K^+ attenuated the vSFG response the least, followed by Na^+, while Li^+ caused the largest attenuation (Figure 1A). Although addition of divalent cations caused a slight increase of the vSFG intensity compared to the neat pH 4 H_2O, the response for the positive alumina/water interface is consistent with the notion that cations are not electrostatically attracted toward a positive interface. However, significant differences are still observed between the monovalent and divalent cations, suggesting unique mechanisms for the interfacial structuring induced by cations, which are discussed below.

The energetics of ion adsorption is complex and dependent on the competing ion/water, water/water, and surface/water interactions. Because different ions have different solvation energies, they tend to have a variable surface affinity. Whenever an ion adsorbs on the interface, it can be partially or completely solvated by interfacial water and/or surface hydroxyl groups. Ions close to a charged surface will screen the opposite surface charge and can also perturb the interfacial hydrogen bonding environment. Both effects are bound to alter the vSFG signal. Historically, the screening effect has been thought to be the primary reason for the ion-induced modulation in the vSFG signal.[10,52,53] However, studies have argued that the changes in the vSFG signal cannot be simply explained by screening effects and that ion-induced reorganization of the interfacial hydrogen bonding environment should be considered.[30,32,54] Recently, divalent cations such as Ca^{2+} and Mg^{2+} have been observed to adsorb more readily on hydrated gibbsite surfaces (α-$Al(OH)_3$) than Na^+ at a wide range of bulk pH values.[55] High-resolution atomic force microscopy and density functional theory confirmed that divalent cations were not only able to screen the charge in the electrical double layer, but their adsorption leads to significant structural changes in the interfacial region.[55] Therefore, it is critical to consider both effects (screening and changes in the interfacial hydrogen bonding environment) to explain the changes in the vSFG signal observed here.

At a positively charged interface (pH 4), anions are expected to be closer to the interface than the cations. Cl^- is the common anion in all the salts added in our experiments. However, differences are still observed in the vSFG signal that can be attributed to the cation effect. In the case of monovalent cations, the vSFG signal is attenuated in the sequence $Cs^+ \approx K^+ < Na^+ < Li^+$ (Figure 1A). Li^+ has the smallest ionic radius which we hypothesize allows it to reside closer to the positively charged interface. A similar trend was observed for halogen anions at the α-$Al_2O_3(0001)/H_2O$ interface, suggesting that the ion charge density plays an important role in efficient screening of positive surface charges.[36]

In contrast, the divalent cations cause a larger vSFG response compared to neat pH 4 water conditions (Figure 1A). This increase in the vSFG signal could be attributed to the higher affinity of divalent cation−Cl^- ion pairs for the interface. The resulting local concentration gradient could lead to an amplified interfacial positive charge and increased vSFG probing depth. This would explain the growth in the magnitude of the vSFG signal. It is worth mentioning that the vSFG spectral shape remains the same for all monovalent and divalent cations at pH 4 condition. This could suggest that the cations near the positively charged alumina surface do not rearrange the interfacial hydrogen bonding environment to a large extent.

Monovalent and divalent cations also have contrasting effects on the interfacial water structure next to a negatively charged alumina surface (Figure 1B), where cations are electrostatically attracted toward the interfacial region. Upon accumulation at the interface, cations are expected to alter the structure of the interfacial region and screen surface charges. These two effects impact the vSFG signal. For the monovalent cations, there is a large attenuation of the vSFG signal at pH 10 similar to our recently observed halide salt effect.[36] In contrast, divalent cations increase the amplitude of the weakly hydrogen-bonded region (~3400 cm^{-1}) with a decreasing cation radius, and for Sr^{2+} and Ca^{2+}, the spectral amplitude in this region is greater than that of neat pH 10 H_2O. This increase in the signal near the 3400 cm^{-1} region is reminiscent of the effect observed at the hydrophobic air/water interface.[30] This is quite surprising because the alumina/water interface is known to be hydrophilic in nature.[56,57] Moreover, the spectral shape of the vSFG is vastly different in the case of monovalent versus divalent cations (Figure 1B), which is discussed below. Overall, we can conclude that the local structure of interfacial water is altered differently by monovalent and divalent cations. These changes in the vSFG signal also cannot be explained by the simple screening effect of cations and a more complex mechanism such as restructuring of the interfacial hydrogen bonding environment must be invoked.

Further analysis of cation effects at the negatively charged α-$Al_2O_3(0001)/H_2O$ interface shows that the valence state of the cations greatly influences the vSFG spectral shape. Under neat pH 10 water conditions, the spectral intensity at 3200 cm^{-1} is greater than that at 3400 cm^{-1}. In the presence of monovalent cations, the vSFG signal is largely attenuated but the 3200 cm^{-1} species is still observed. However, the ~3400 cm^{-1} peak appears to be missing. This observation is consistent with our previous study where we investigated the effect of sodium halide salts next to a negatively charged alumina surface.[36] In contrast, when divalent cations are introduced, the spectral intensity at 3400 cm^{-1} is enhanced and the 3200 cm^{-1} peak is attenuated. Upon further inspection, vSFG spectra in the presence of divalent cations at the negatively charged alumina surface display similar spectral profiles to the vSFG spectra recorded at the positively charged alumina surface, albeit with discrepancies in the ~3200 cm^{-1} peak intensities. The similarity in vSFG spectral profiles for divalent cations at pH 4 and pH 10 suggests that the divalent cations at the negatively charged alumina surface induce orientational flipping of surface water molecules such that interfacial water molecules are arranged with the oxygen atoms closer to the alumina surface compared to the neat pH 10 vSFG spectra (where we expect a hydrogen atom pointing toward the negative alumina surface). This flipping of surface water molecules and the large magnitude of the divalent cation solution vSFG response compared to pH 10 H_2O was unexpected, and marks the difference in induced changes in the orientation of interfacial

DOI: 10.1021/acs.jpcc.9b01618
J. Phys. Chem. C 2019, 123, 18315−18324

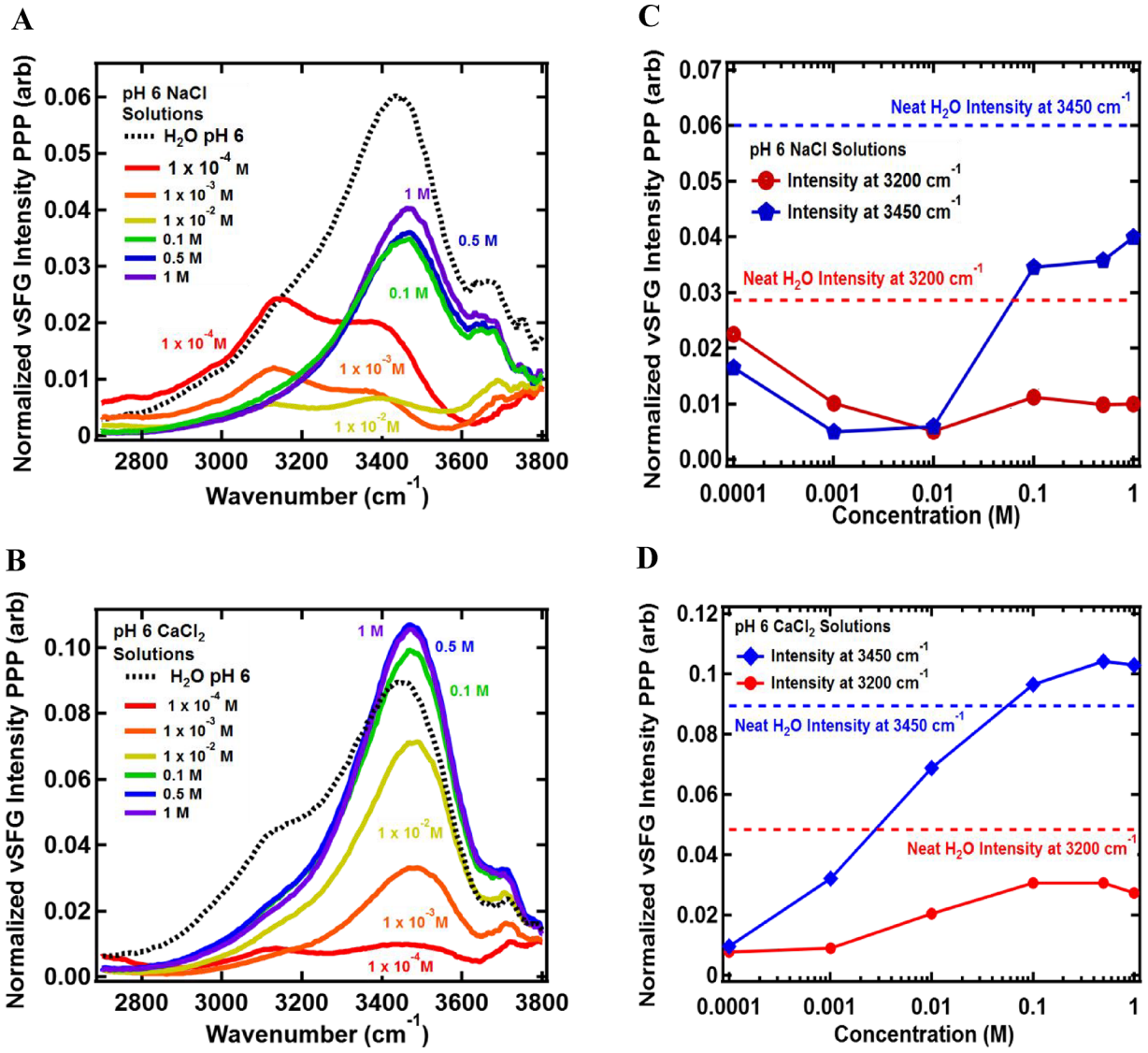

Figure 2. Concentration dependence of the vSFG spectra at pH 6 for (A) NaCl and (B) $CaCl_2$ for PPP polarization. Dotted spectra show neat pH 6 H_2O. The normalized intensity (not extracted from fitting) vs concentration of the strong (~3200 cm^{-1}) and weak (~3400 cm^{-1}) for (C) NaCl and (D) $CaCl_2$ is shown on the right-hand side. For divalent $CaCl_2$ at high enough salt concentration, the vSFG signal is larger than pure water in contrast to monovalent NaCl.

water molecules by monovalent cations compared to divalent cations.

The vSFG spectra of $CaCl_2$ and CsCl at the negatively charged surface were fit using a sum of Lorentzian lineshapes.[58] The details of the model and parameters used can be found in the Supporting Information (Figure S2). The fitting results show that the weakly hydrogen-bonded species at ~3400 cm^{-1} in monovalent spectra have an opposite relative orientation compared to that of the surface aluminol groups (3700 cm^{-1}), while the ~3400 cm^{-1} species in divalent spectra at pH 10 share the same relative orientation as that of the surface aluminol group, providing further evidence of interfacial water flipping in response to surface charging by the divalent cations. It is important to note that previous theoretical studies have assigned the ~3700 cm^{-1} species of the α-$Al_2O_3(0001)/H_2O$ interface to out of plane aluminol groups, making this inference possible.[23] Future experimental studies, such as previously performed at the α-$Al_2O_3(11\bar{2}0)/H_2O$, are required to better understand the origin of the ~3700 cm^{-1} species at the α-$Al_2O_3(0001)/H_2O$ interface.[40] The change in the orientation of the ~3400 cm^{-1} species is discussed further in the next section while analyzing the cation concentration dependence.

The repeated observation of more spectral intensity in the weakly hydrogen-bonded region (~3400 cm^{-1}) than for neat pH 10 H_2O after the addition of divalent cations is evidence that such cations do not merely screen the interfacial charge but actively rearrange the interfacial hydrogen bonding network at the negatively charged interface. The ~3200 cm^{-1} region in divalent cation spectra at pH 10 likely comes from water molecules closest to the interface because of the strong stabilization of the H-bonds from aluminol groups.[23] This suggests that divalent cations are overcharging the interface, leading to a larger spectral contribution from water in the diffuse layer signal originating at ~3400 cm^{-1}, and may be the reason that we observe a greater change in the net orientation of water at the negatively charged surface compared to the positive or neutral surfaces. The ability to increase the vSFG response compared to neat pH 4 and pH 10

DOI: 10.1021/acs.jpcc.9b01618
J. Phys. Chem. C 2019, 123, 18315−18324

H_2O shows that divalent cations lead to a more oriented interfacial solvent and accomplish this by charging the interface leading to a longer vSFG active region. Alternatively, divalent cations could also induce more ordering in the Stern layer which would also increase the vSFG signal, but we expect this increase to occur in the 3200 cm^{-1} region (and not at the experimentally observed 3400 cm^{-1} region) as per our assignment of the vSFG spectra.

To investigate the differences in surface affinity of monovalent versus divalent cations, vSFG spectra of NaCl and $CaCl_2$ were measured over a wide concentration range. While our vSFG spectra versus concentration for monovalent and divalent salts were not measured at the same ionic (Figure 2) strength, the cation concentration in each case is equal. The vSFG spectra in the 1×10^{-4} M to 1 M range at the nominally uncharged α-$Al_2O_3(0001)/H_2O$ interface display an initial decrease in the vSFG intensity upon the addition of NaCl and $CaCl_2$. As the cation concentration is increased, Na^+ continues to decrease the vSFG intensity in the ~3200 and ~3450 cm^{-1} regions until 1×10^{-2} M, while the Ca^{2+} increases the vSFG intensity for both peaks in this concentration regime. The vSFG intensity at ~3450 cm^{-1}, rather than ~3400 cm^{-1}, was chosen for the weakly hydrogen-bonded species because a slight blue shift was observed for both NaCl and $CaCl_2$ as the concentration is increased, making ~3450 cm^{-1} more representative of the spectral response. At concentrations greater than 1×10^{-2} M for both Na^+ and Ca^{2+}, the ~3200 cm^{-1} species reaches an asymptotic limit while the ~3450 cm^{-1} feature continues to grow until ~0.5 M. This asymptotic attenuation of strongly hydrogen-bonded species is consistent with an interfacial picture consisting of adjacent surface species contributing at ~3200 cm^{-1}, because of the limited number of surface sites compared to the volume of the diffuse layer.

While high concentrations of both monovalent and divalent cations at pH 6 lead to similar spectral shapes, both exhibit unique surface affinities manifested in the modulation of the vSFG response. An important distinction in the adsorption behavior of Na^+ and Ca^{2+} is that at high concentrations, the absolute intensity of the divalent cation vSFG spectra is greater than that of the electrolyte-free pH 6 water while the vSFG signal for the monovalent cations is still lower than the electrolyte-free pH 6 case. The shift in the spectral density from the strongly hydrogen-bonded species (water adjacent to the alumina surface) at ~3200 cm^{-1} to weakly hydrogen-bonded species (water in the diffuse layer) at ~3400 cm^{-1} is observed at concentrations as low as 1×10^{-3} M for $CaCl_2$ and is not seen until 0.1 M for NaCl. This suggests that divalent Ca^{2+} accumulates more rapidly at the neutral surface, as a higher concentration of Na^+ is required to achieve a similar vSFG spectral profile. This increase in the spectral response in the ~3400 cm^{-1} region likely arises from an increased contribution from the diffuse layer, facilitated by the adsorption of divalent cations which can lead to the accumulation of a net surface charge at a nominally neutral surface. The earlier onset of interfacial charging seen for $CaCl_2$ vSFG spectra compared to NaCl spectra indicates that divalent cations have a greater affinity for, and accumulate more rapidly at, the uncharged α-$Al_2O_3(0001)/H_2O$ interface than monovalent cations.

Previous investigations of the concentration dependence of the SiO_2/H_2O interface vSFG response showed a minimum at low NaCl concentrations (10^{-7} to 10^{-5} M) followed by a maximum (10^{-3} M) and finally another low response region at higher NaCl concentrations (10^{-1} to 10 M).[45] Recent studies have pointed the constructive and deconstructive interference between the diffuse layer and Stern layer contributions to the vSFG response to explain the changes in the spectral intensity with varying electrolyte concentration.[44,45,59] Modulations of the $\chi^{(3)}$ contribution and the interfacial potential in current models only consider the ionic strength, which does not account for ion identity. The observation that different ions change the vSFG intensity with almost no affect in the spectral shape suggests that that specific ion effects on the interfacial potential need to be considered.

As the structure of interfacial water is related to its ability to redistribute vibrational energy, TR-vSFG was employed to see if the structural changes of the interfacial water hydrogen bonding network induced by cations were mirrored in the timescale of vibrational relaxation.[60] TR-vSFG experiments can determine the vibrational lifetimes of the O−H stretch, a parameter indicative of the local hydrogen bond network strength.[38] The kinetics of the excited O−H stretches to their ground states is modeled using a four-level model comprising two time scales: a vibrational lifetime (T_1) and thermalization (T_{th}).[38,39,48,61,62] The relaxation of the excited O−H stretch mode from the first excited state ($\nu = 1$) to an intermediate state ($\nu = \nu^*$), typically ascribed to the overtone of the water bending mode, is denoted by T_1.[1,42,63] The time required for the subsequent relaxation from the intermediate ($\nu = \nu^*$) state to a hot ground state ($\nu = 0^*$) is represented by T_{th}. The model used to fit the TR-vSFG data is described in the Supporting Information. The extracted T_1 lifetimes in this work are similar to those in our previous study for pH 4 and pH 10 aqueous environments.[38] At the positively charged alumina surface, the T_1 lifetimes for interfacial water in the presence of 0.1 M NaCl and $BaCl_2$ are indistinguishable within the uncertainty of our fitting (Figure 3). TR-vSFG spectra of all cations presented in Figure 1 were also recorded, and monovalent cations and divalent cations behaved similarly to Na^+ and Ba^{2+} (Figure S4). While the extracted T_1 lifetimes are also similar near the negatively charged surface, the population of molecules that return to their original state (indicated by the normalized vSFG intensity) is affected by NaCl and $BaCl_2$ indicating that structural changes can be tracked using TR-vSFG.

Because the structure of interfacial water affects its vibrational dynamics, similar TR-vSFG spectra for monovalent and divalent cations at the positively charged interface are not surprising, reflecting the similarities in the vSFG spectral shape for both species at pH 4 condition (Figure 1). As the steady-state vSFG spectra at pH 4 contain approximately the same relative amplitudes of the strongly and weakly hydrogen-bonded species at ~3200 and ~3400 cm^{-1}, the ability for both interfacial environments to redistribute vibrational energy may remain constant. We hypothesize that divalent cations accumulate more readily at the positively charged surface via a Cl^- counter ion divalent cation interaction and their presence leads to an enhanced spectral intensity at pH 4 (Figure 1), reflecting increased ordered interfacial water. This slight enhancement of the interfacial water structure indicated by steady-state vSFG, however, is not enough to change the interfacial vibrational dynamics indicated by the T_1 lifetime.

The large changes in the static vSFG spectral shape induced by monovalent and divalent cations at the negatively charged alumina surface suggested that the vibrational dynamics of the O−H modes in each environment would be quite different.

DOI: 10.1021/acs.jpcc.9b01618
J. Phys. Chem. C 2019, 123, 18315−18324

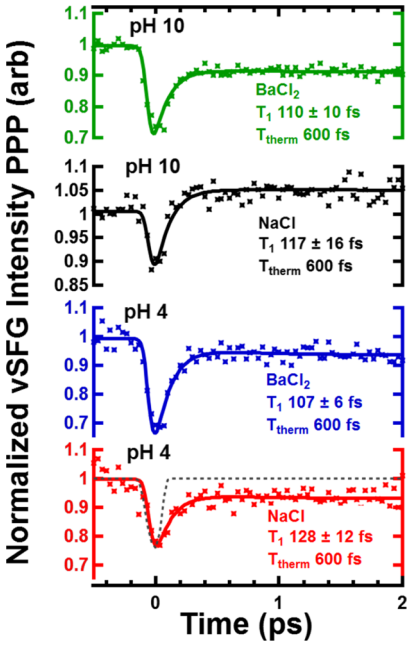

Figure 3. Time-resolved vSFG spectra of 0.1 M NaCl and 0.1 M $BaCl_2$ at pH 4 and pH 10 recorded in the PPP geometry. The third-order cross-correlation between the IR pump, IR probe, and visible probe is shown by the black dashed line and has a fwhm of ∼105 fs, suggesting IR pulse durations of ∼75 fs. T_1 lifetimes are extracted from a four-level model described in the Supporting Information.

However, even though the H-bond strength is typically correlated with ordering of the H-bond network, there is no change in T_1 lifetimes for the pH 10 TR-vSFG spectra (Figure 3). At the α-$Al_2O_3(0001)/H_2O$ interface, only F^- has shown the ability to slow the vibrational dynamics of water near the surface, and these slower dynamics resulted from strong contact adsorption of F^-.[36] While monovalent and divalent cations are able to rearrange interfacial water species at pH 10, they do not appear to be able to interrupt strong hydrogen bonding between the alumina surface and adjacent water molecules, resulting in similar T_1 lifetimes for all cations tested here.

The final versus initial normalized vSFG intensities, however, do vary for TR-vSFG of $BaCl_2$ and NaCl solutions. For $BaCl_2$, the vSFG intensity is lower post bleach (∼90% of the original intensity), and we attribute this to the formation of less-strongly hydrogen-bonded species post excitation due to an increase in local temperature induced by the strong IR pump pulse. Because our pump and probe IR pulses contain ∼250 cm^{-1} of bandwidth [full width at half-maximum (fwhm)] centered at ∼3150 cm^{-1}, newly formed weakly hydrogen bonded species are likely to have a natural frequency outside our probe window. TR-vSFG spectra of NaCl contain more vSFG intensity in the probe window after the spectral bleach (∼105% of original intensity), indicating that more species in the strongly hydrogen-bonded region (∼3200 cm^{-1}) have been formed. While the extracted T_1 lifetimes at pH 10 for both monovalent and divalent cations are similar, the differences in the steady-state vSFG spectral shape at pH 10 lead to different amounts of recovered strongly hydrogen-bonded populations, indicated by the magnitude of the normalized vSFG response post excitation. This suggests that an alternative relaxation mechanism is available to interfacial water in the presence of monovalent cations at pH 10. However, it is impossible to understand the exact nature of this mechanism from our experiments alone.

To understand differences in vibrational relaxation pathways after excitation by the pump pulse at pH 10 condition, we analyze the steady-state vSFG spectra for insight. vSFG spectra of pH 10 monovalent cations revealed that the ∼3400 cm^{-1} species has an opposite relative orientation (Figure S2) to out of plane surface aluminol groups and the ∼3400 cm^{-1} species observed in divalent spectra at pH 10.[23] The interfacial depth is also much smaller when the surface is screened by monovalent cations at pH 10, shown by the larger degree of attenuation in vSFG spectra. Previously, we speculated that the recovery of the vSFG response in the presence of monovalent halide salts was correlated with the large attenuation in the vSFG signal in the steady-state spectra.[36] The addition of divalent salts increases the vSFG intensity at the negatively charged surface, and does not show recovery to the initial vSFG response. It seems that the steady-state vSFG response is crucial to understand the differences in vibrational dynamics displayed here, although the origin of the correlation is unclear.

After careful consideration of the steady-state vSFG spectra, the surface affinities Na^+ and Ca^{2+}, and the vibrational dynamics of the interface, we can hypothesize the interfacial arrangement of water molecules at the α-$Al_2O_3(0001)$ surface. For both positively and negatively charged alumina surfaces, divalent cations seem to have greater affinity for the interface compared to the monovalent cations. Under positively charged alumina surface conditions, Cl^- attenuates the vSFG response with varied effectiveness correlated with the ionic radius of the counter cation, while the higher density of divalent cations near the interface causes an increase in the positive surface charge resulting in more vSFG intensity than neat pH 4 H_2O. In the case of negatively charged alumina surfaces, the screening of the interfacial potential by monovalent cations leads to a short vSFG active interfacial region, shown by the high degree of attenuation of spectra at pH 10 compared to neat pH 10 H_2O (Figure 1). Divalent cations are more attracted to the interface and initially screen the interfacial charge generated by deprotonated aluminol groups. Additional ions are then drawn toward the interface and accumulate, overcharging the interface and increasing the number of aligned water molecules in the diffuse layer, which results in an increase in the amplitude of the ∼3450 cm^{-1} region. Concentration-dependent vSFG spectra also suggest that divalent cations adsorb more than monovalent cations at the uncharged alumina surface (Figure 2). It should be noted that spectra recorded at higher concentrations of NaCl (>0.1 M) tend to resemble $CaCl_2$ spectra, with much of the spectral intensity coming from the weakly hydrogen-bonded region. The increase of the spectral intensity in the weakly hydrogen-bonded region, however, has an earlier onset for $CaCl_2$ (0.001 M) suggesting that divalent cations have a higher affinity than Na^+ for the alumina/water interface. One explanation for the difference in adsorption affinities for these two ions could be the strong electrostatic interaction between divalent cations and surface oxygen atoms of mineral oxide surfaces previously observed in X-ray spectroscopic measurements.[64−67] Although the Ca^{2+} and Na^+ hydration energies, −1579 and −406 kJ/mol, respectively, indicate that Ca^{2+} is less likely to perturb its hydration shell upon adsorption, the stabilization by surface hydroxyl groups appears to overcome this thermodynamic barrier, leading to the higher adsorption affinity seen for divalent cations.[68]

DOI: 10.1021/acs.jpcc.9b01618
J. Phys. Chem. C 2019, 123, 18315−18324

All of these observations can be coupled into a schematic (Figure 4) which displays the hypothesized interfacial

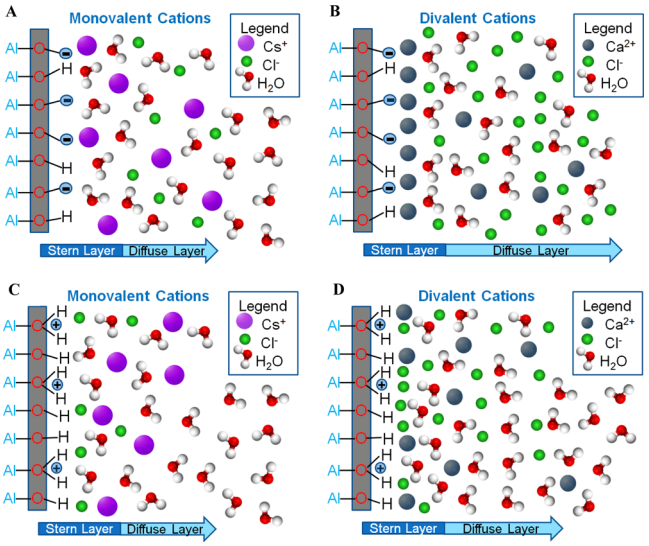

Figure 4. Schematic of the hypothesized interfacial water arrangement at the negatively charged α-$Al_2O_3(0001)/H_2O$ interface in the presence of (A) monovalent cations and (B) divalent cations at 0.1 M electrolyte concentration and the positively charged interface in the presence of (C) monovalent cations and (D) divalent cations at 0.1 M.

organization of the α-$Al_2O_3(0001)/H_2O$ interface in the presence of (A,C) monovalent cations and (B,D) divalent cations at 0.1 M electrolyte concentration. We, therefore, find that specific ion effects play a large role in altering the interfacial water arrangement and hence the vSFG at the α-$Al_2O_3(0001)/H_2O$ interface, and encourage further investigation of this interface via computational efforts.

CONCLUSIONS

Steady-state and time-resolved vSFG measurements of the α-$Al_2O_3(0001)/H_2O$ interface and their dependence on cation identity, concentration, and surface charge were investigated to better understand how cations affect the structure and vibrational dynamics of interfacial water. In addition to passive charge screening by ions at other solid/liquid interfaces, monovalent and divalent cations were able to induce reorganization of surface water at the α-$Al_2O_3(0001)/H_2O$ interface.[31,33] Monovalent cations at pH 4 attenuated the vSFG response which we attribute to passive screening of surface charges. At positive surface charge, we hypothesize that the higher surface affinity of divalent cations allows them to charge the interface resulting in a larger vSFG response. At the negatively charged surface, monovalent cations attenuate the vSFG response and orient the ~3200 cm^{-1} species with oxygen atoms toward the surface and the ~3400 cm^{-1} species with hydrogen atoms toward the surface. In contrast, strongly hydrogen-bonded and weakly hydrogen-bonded species share the same net orientation as aluminol groups for divalent vSFG spectra. Divalent cation spectra are dominated by the ~3400 cm^{-1} species, and for Sr^{2+} and Ca^{2+}, the spectral amplitude is greater than neat pH 10 H_2O. The ion specificity of interfacial accumulation and hence charging, especially for divalent cations at the negatively charged surface, are not accounted for in current models that describe the interfacial potential via electrolyte concentration only.[44,45]

Concentration-dependent vSFG spectra showed that divalent cations have a greater affinity for the neutral interface than monovalent cations, a characteristic that could lead to selective alkaline filtration technologies. Divalent cations also increase vSFG signals in the weakly hydrogen bonding region (~3400 cm^{-1}) to greater amplitudes than neat water of the same pH value, suggesting that passive screening is not sufficient to explain the behavior of divalent cations at the alumina/liquid interface. At high (~1 M) concentrations, monovalent cations reached similar vSFG amplitudes of neat water. The large difference in adsorption affinities for Na^+ and Ca^{2+} suggests that Ca^{2+} more readily loses its hydration shell allowing for easier access to the surface and consequent overcharging of the interfacial region.

Lastly, time-resolved vSFG measurements at the positively (pH 4) and negatively (pH 10) charged interfacial region were taken to capture changes in the vibrational dynamics of interfacial water populations solvating monovalent and divalent cations. These measurements revealed that cation identity and bulk pH have surprisingly little influence on the T_1 lifetime, suggesting that regardless of the restructuring of the interfacial region, sufficient channels to redistribute vibrational energy in an ultrafast manner exist due to the vibrational density of states available in the ~3000 cm^{-1} region. Monovalent and divalent cations lead to similar TR-vSFG response at pH 4, but at the negatively charged interface, monovalent cations lead to an increase in the strongly hydrogen-bonded population after excitation at ~3200 cm^{-1} while water solvating divalent cations recover to a smaller vSFG intensity than pre-excitation. We attribute the increase in strongly hydrogen-bonded population to the observed oxygen down orientation of the strongly hydrogen-bonded species in the presence of monovalent cations, which reduces hydrogen bonding with the oppositely oriented weakly hydrogen-bonded species in the diffuse layer. This reduced coupling implies that after strongly hydrogen-bonded species interacting with surface aluminols (~3000−3100 cm^{-1}) are disrupted by the pump pulse, they are more likely to form hydrogen bonds with a natural frequency near ~3200 cm^{-1} as sampled by the probe pulse centered at ~3150 cm^{-1}. The SFG response for divalent cations does not recover to the initial value suggesting that the excited O−H species relax into vibrational states that have a natural frequency outside our spectral window. This highlights that those large structural changes of the interface seen in steady-state vSFG spectra manifest themselves in the TR-vSFG spectra. Our results reveal critical insight on how monovalent and divalent cations uniquely alter the structure and vibrational dynamics of the α-$Al_2O_3(0001)/H_2O$ interface. These findings provide crucial insight, which will aid in obtaining a molecular-level view of electric double layers, which have been a challenging subject in the field of interfacial science.

ASSOCIATED CONTENT

Supporting Information

The Supporting Information is available free of charge on the ACS Publications website at DOI: 10.1021/acs.jpcc.9b01618.

1. Comparison of monovalent and divalent spectral profiles at pH 4 conditions. 2 Fitting of steady state vSFG data. 3 Four level model used to fit time resolved vSFG dynamics. 4. Limitations of the four level model. 5.

DOI: 10.1021/acs.jpcc.9b01618
J. Phys. Chem. C 2019, 123, 18315−18324

Fitting parameters for time-resolved vSFG data in figure 3. 6. Time resolved vSFG Spectra of other mono and divalent cations. 7. Integration times for steady state and time resolved vSFG data. 8. Elements of nonlinear susceptibility probed using PPP experimental geometry (PDF)

AUTHOR INFORMATION

Corresponding Author

*E-mail: eborguet@temple.edu.

ORCID

Stefan M. Piontek: 0000-0001-9564-6258

Aashish Tuladhar: 0000-0003-2449-4984

Notes

The authors declare no competing financial interest.

ACKNOWLEDGMENTS

The authors acknowledge the National Science Foundation for supporting this work (NSF grant CHE 1828421). A.T. also acknowledges the support provided by the US Department of Energy (DOE), Office of Science, Office of Basic Energy Sciences, Division of Materials Science and Engineering at Pacific Northwest National Laboratory (PNNL). The authors also thank Professor M. Zdilla (Temple University, Chemistry Department) for alumina prism face orientation identification via X-ray diffraction and Dr. Kyle Gilroy, (Professor S. Neretina Group, Temple University, College of Engineering) for gold coating our alumina prisms.

REFERENCES

(1) Smits, M.; Ghosh, A.; Bredenbeck, J.; Yamamoto, S.; Müller, M.; Bonn, M. Ultrafast Energy Flow in Model Biological Membranes. *New J. Phys.* **2007**, *9*, 390.

(2) Bucher, D.; Kuyucak, S. Polarization of Water in the First Hydration Shell of K^+ and Ca^{2+} Ions. *J. Phys. Chem. B* **2008**, *112*, 10786−10790.

(3) Cygan, R. T.; Liang, J.-J.; Kalinichev, A. G. Molecular Models of Hydroxide, Oxyhydroxide, and Clay Phases and the Development of a General Force Field. *J. Phys. Chem. B* **2004**, *108*, 1255−1266.

(4) Joung, I. S.; Cheatham, T. E. Molecular Dynamics Simulations of the Dynamic and Energetic Properties of Alkali and Halide Ions Using Water-Model-Specific Ion Parameters. *J. Phys. Chem. B* **2009**, *113*, 13279−13290.

(5) Lee, S. H.; Rasaiah, J. C. Molecular Dynamics Simulation of Ion Mobility. 2. Alkali Metal and Halide Ions Using the SPC/E Model for Water at 25° C. *J. Phys. Chem.* **1996**, *100*, 1420−1425.

(6) Bakker, H. J.; Kropman, M. F.; Omta, A. W. Effect of Ions on the Structure and Dynamics of Liquid Water. *J. Phys.: Condens. Matter* **2005**, *17*, S3215−S3224.

(7) Kropman, M. F.; Bakker, H. J. Vibrational Relaxation of Liquid Water in Ionic Solvation Shells. *Chem. Phys. Lett.* **2003**, *370*, 741−746.

(8) Li, R.; Jiang, Z.; Chen, F.; Yang, H.; Guan, Y. Hydrogen Bonded Structure of Water and Aqueous Solutions of Sodium Halides: A Raman Spectroscopic Study. *J. Mol. Struct.* **2004**, *707*, 83−88.

(9) Näslund, L.-Å.; Edwards, D. C.; Wernet, P.; Bergmann, U.; Ogasawara, H.; Pettersson, L. G. M.; Myneni, S.; Nilsson, A. X-ray Absorption Spectroscopy Study of the Hydrogen Bond Network in the Bulk Water of Aqueous Solutions. *J. Phys. Chem. A* **2005**, *109*, 5995−6002.

(10) Du, Q.; Freysz, E.; Shen, Y. R. Vibrational Spectra of Water Molecules at Quartz/Water Interfaces. *Phys. Rev. Lett.* **1994**, *72*, 238−241.

(11) Ong, S.; Zhao, X.; Eisenthal, K. B. Polarization of Water-Molecules at a Charged Interface—2nd Harmonic Studies of the Silica Water Interface. *Chem. Phys. Lett.* **1992**, *191*, 327−335.

(12) Kelber, J. Alumina Surfaces and Interfaces Under Non-Ultrahigh Vacuum Conditions. *Surf. Sci. Rep.* **2007**, *62*, 271−303.

(13) Sang, Y.; Gu, Q.; Sun, T.; Li, F.; Liang, C. Filtration by a Novel Nanofiber Membrane and Alumina Adsorption to Remove Copper-(II) from Groundwater. *J. Hazard. Mater.* **2008**, *153*, 860−866.

(14) Korhonen, H.; Syväluoto, A.; Leskinen, J. T. T.; Lappalainen, R. Optically Transparent and Durable Al_2O_3 Coatings for Harsh Environments by Ultra Short Pulsed Laser Deposition. *Opt. Laser Technol.* **2018**, *98*, 373−384.

(15) Ha, J.-H.; Lee, S.; Choi, J. R.; Lee, J.; Song, I.-H.; Lee, S. J.; Choi, J. Development of a Carbon-Coated Reticulated Porous Alumina Material with Tailored Structural Properties for Potential Radar-Absorption Applications. *Ceram. Int.* **2017**, *43*, 16924−16930.

(16) Sun, R.; Yao, H.; Zhang, H.-B.; Li, Y.; Mai, Y.-W.; Yu, Z.-Z. Decoration of Defect-Free Graphene Nanoplatelets with Alumina for Thermally Conductive and Electrically Insulating Epoxy Composites. *Compos. Sci. Technol.* **2016**, *137*, 16−23.

(17) Catalano, J. G. Weak Interfacial Water Ordering on Isostructural Hematite and Corundum (001) Surfaces. *Geochim. Cosmochim. Acta* **2011**, *75*, 2062−2071.

(18) de Leeuw, N. H.; Parker, S. C. Effect of Chemisorption and Physisorption of Water on the Surface Structure and Stability of α-Alumina. *J. Am. Ceram. Soc.* **1999**, *82*, 3209−3216.

(19) Elam, J. W.; Nelson, C. E.; Cameron, M. A.; Tolbert, M. A.; George, S. M. Adsorption of H_2O on a Single-Crystal α-Al_2O_3(0001) Surface. *J. Phys. Chem. B* **1998**, *102*, 7008−7015.

(20) Eng, P. J.; Trainor, T. P.; Brown, G. E.; Waychunas, G. A.; Newville, M.; Sutton, S. R.; Rivers, M. L. Structure of the Hydrated α-Al_2O_3 (0001) Surface. *Science* **2000**, *288*, 1029−1033.

(21) Hass, K. C.; Schneider, W. F.; Curioni, A.; Andreoni, W. First-Principles Molecular Dynamics Simulations of H_2O on α-Al_2O_3 (0001). *J. Phys. Chem. B* **2000**, *104*, 5527−5540.

(22) Liu, P.; Kendelewicz, T.; Brown, G. E.; Nelson, E. J.; Chambers, S. A. Reaction of Water Vapor with α-Al_2O_3(0001) and α-Fe_2O_3(0001) Surfaces: Synchrotron X-Ray Photoemission Studies and Thermodynamic Calculations. *Surf. Sci.* **1998**, *417*, 53−65.

(23) Gaigeot, M.-P.; Sprik, M.; Sulpizi, M. Oxide/Water Interfaces: How the Surface Chemistry Modifies Interfacial Water Properties. *J. Phys.: Condens. Matter* **2012**, *24*, 124106.

(24) DelloStritto, M.; Piontek, S. M.; Klein, M. L.; Borguet, E. Relating Interfacial Order to Sum Frequency Generation with Ab Initio Simulations of the Aqueous Al_2O_3(0001) and (1120) Interfaces. *J. Phys. Chem. C* **2018**, *122*, 21284−21294.

(25) Sung, J.; Shen, Y. R.; Waychunas, G. A. The Interfacial Structure of Water/Protonated α-Al_2O_3 (1120) as a Function of pH. *J. Phys.: Condens. Matter* **2012**, *24*, 124101.

(26) Yeganeh, M. S.; Dougal, S. M.; Pink, H. S. Vibrational Spectroscopy of Water at Liquid/Solid Interfaces: Crossing the Isoelectric Point of a Solid Surface. *Phys. Rev. Lett.* **1999**, *83*, 1179−1182.

(27) Zhang, L.; Tian, C.; Waychunas, G. A.; Shen, Y. R. Structures and Charging of α-Alumina (0001)/Water Interfaces Studied by Sum-Frequency Vibrational Spectroscopy. *J. Am. Chem. Soc.* **2008**, *130*, 7686−7694.

(28) Covert, P. A.; Hore, D. K. Geochemical Insight from Nonlinear Optical Studies of Mineral-Water Interfaces. In *Annual Review of Physical Chemistry, Vol 67*; Johnson, M. A., Martinez, T. J., Eds.; Annual Reviews, 2016; Vol. 67, pp 233−257.

(29) Heginbotham, L.; Abramson, T.; Mackinnon, R. A Functional Connection Between the Pores of Distantly Related Ion Channels As Revealed by Mutant K^+ Channels. *Science* **1992**, *258*, 1152−1155.

(30) Xu, M.; Spinney, R.; Allen, H. C. Water Structure at the Air-Aqueous Interface of Divalent Cation and Nitrate Solutions. *J. Phys. Chem. B* **2009**, *113*, 4102−4110.

DOI: 10.1021/acs.jpcc.9b01618
J. Phys. Chem. C 2019, 123, 18315−18324

(31) Yang, Z.; Li, Q.; Chou, K. C. Structures of Water Molecules at the Interfaces of Aqueous Salt Solutions and Silica: Cation Effects. *J. Phys. Chem. C* **2009**, *113*, 8201−8205.
(32) Dewan, S.; Yeganeh, M. S.; Borguet, E. Experimental Correlation Between Interfacial Water Structure and Mineral Reactivity. *J. Phys. Chem. Lett.* **2013**, *4*, 1977−1982.
(33) Flores, S. C.; Kherb, J.; Konelick, N.; Chen, X.; Cremer, P. S. The Effects of Hofmeister Cations at Negatively Charged Hydrophilic Surfaces. *J. Phys. Chem. C* **2012**, *116*, 5730−5734.
(34) Romero, C.; Moore, H. J.; Lee, T. R.; Baldelli, S. Orientation of 1-Butyl-3-Methylimidazolium Based Ionic Liquids at a Hydrophobic Quartz Interface Using Sum Frequency Generation Spectroscopy. *J. Phys. Chem. C* **2007**, *111*, 240−247.
(35) Lovering, K. A.; Bertram, A. K.; Chou, K. C. New Information on the Ion-Identity-Dependent Structure of Stern Layer Revealed by Sum Frequency Generation Vibrational Spectroscopy. *J. Phys. Chem. C* **2016**, *120*, 18099−18104.
(36) Tuladhar, A.; Piontek, S. M.; Frazer, L.; Borguet, E. Effect of Halide Anions on the Structure and Dynamics of Water Next to an Alumina (0001) Surface. *J. Phys. Chem. C* **2018**, *122*, 12819−12830.
(37) Hsieh, C.-S.; Okuno, M.; Hunger, J.; Backus, E. H. G.; Nagata, Y.; Bonn, M. Aqueous Heterogeneity at the Air/Water Interface Revealed by 2D-HD-SFG Spectroscopy. *Angew. Chem., Int. Ed.* **2014**, *53*, 8146−8149.
(38) Tuladhar, A.; Piontek, S. M.; Borguet, E. Insights on Interfacial Structure, Dynamics, and Proton Transfer from Ultrafast Vibrational Sum Frequency Generation Spectroscopy of the Alumina(0001)/Water Interface. *J. Phys. Chem. C* **2017**, *121*, 5168−5177.
(39) Tuladhar, A.; Dewan, S.; Kubicki, J. D.; Borguet, E. Spectroscopy and Ultrafast Vibrational Dynamics of Strongly Hydrogen Bonded OH Species at the α-Al_2O_3(1120)/H_2O Interface. *J. Phys. Chem. C* **2016**, *120*, 16153−16161.
(40) Boulesbaa, A.; Borguet, E. Vibrational Dynamics of Interfacial Water by Free Induction Decay Sum Frequency Generation (FID-SFG) at the Al_2O_3(1120)/H_2O Interface. *J. Phys. Chem. Lett.* **2014**, *5*, 528−533.
(41) Eftekhari-Bafrooei, A.; Nihonyanagi, S.; Borguet, E. Spectroscopy and Dynamics of the Multiple Free OH Species at an Aqueous/Hydrophobic Interface. *J. Phys. Chem. C* **2012**, *116*, 21734−21741.
(42) Eftekhari-Bafrooei, A.; Borguet, E. Effect of Electric Fields on the Ultrafast Vibrational Relaxation of Water at a Charged Solid-Liquid Interface as Probed by Vibrational Sum Frequency Generation. *J. Phys. Chem. Lett.* **2011**, *2*, 1353−1358.
(43) Wang, R.; DelloStritto, M.; Remsing, R. C.; Carnevale, V.; Klein, M. L.; Borguet, E. Sodium Halide Adsorption and Water Structure at the α-Alumina (0001)/Water Interface. *J. Phys. Chem. C* **2019**, *123*, 15618.
(44) Ohno, P. E.; Wang, H.-f.; Geiger, F. M. Second-Order Spectral Lineshapes from Charged Interfaces. *Nat. Commun.* **2017**, *8*, 1032.
(45) Schaefer, J.; Gonella, G.; Bonn, M.; Backus, E. H. G. Surface-Specific Vibrational Spectroscopy of the Water/Silica Interface: Screening and Interference. *Phys. Chem. Chem. Phys.* **2017**, *19*, 16875−16880.
(46) Aulin, Y. V.; Tuladhar, A.; Borguet, E. Ultrabroadband mid-infrared noncollinear difference frequency generation in a silver thiogallate crystal. *Opt. Lett.* **2018**, *43*, 4402−4405.
(47) Tian, T. S.; Shen, Y. R. Comment on "Vibrational Response of Hydrogen-Bonded Interfacial Water is Dominated by Intramolecular Coupling"—Reply. *Phys. Rev. Lett.* **2008**, *101*, 173901.
(48) Eftekhari-Bafrooei, A.; Borguet, E. Effect of Hydrogen-Bond Strength on the Vibrational Relaxation of Interfacial Water. *J. Am. Chem. Soc.* **2010**, *132*, 3756−3761.
(49) Myalitsin, A.; Urashima, S.-h.; Nihonyanagi, S.; Yamaguchi, S.; Tahara, T. Water Structure at the Buried Silica/Aqueous Interface Studied by Heterodyne-Detected Vibrational Sum-Frequency Generation. *J. Phys. Chem. C* **2016**, *120*, 9357−9363.
(50) Braunschweig, B.; Eissner, S.; Daum, W. Molecular Structure of a Mineral/Water Interface: Effects of Surface NanoRoughness of α-Al_2O_3(0001). *J. Phys. Chem. C* **2008**, *112*, 1751−1754.
(51) Gopalakrishnan, S.; Jungwirth, P.; Tobias, D. J.; Allen, H. C. Air-Liquid Interfaces of Aqueous Solutions Containing Ammonium and Sulfate: Spectroscopic and Molecular Dynamics Studies. *J. Phys. Chem. B* **2005**, *109*, 8861−8872.
(52) Fitts, J. P.; Shang, X.; Flynn, G. W.; Heinz, T. F.; Eisenthal, K. B. Electrostatic Surface Charge at Aqueous/α-Al_2O_3 Single-Crystal Interfaces as Probed by Optical Second-Harmonic Generation. *J. Phys. Chem. B* **2005**, *109*, 7981−7986.
(53) Jena, K. C.; Covert, P. A.; Hore, D. K. The Effect of Salt on the Water Structure at a Charged Solid Surface: Differentiating Second- and Third-order Nonlinear Contributions. *J. Phys. Chem. Lett.* **2011**, *2*, 1056−1061.
(54) Dewan, S.; Carnevale, V.; Bankura, A.; Eftekhari-Bafrooei, A.; Fiorin, G.; Klein, M. L.; Borguet, E. Structure of Water at Charged Interfaces: A Molecular Dynamics Study. *Langmuir* **2014**, *30*, 8056−8065.
(55) Siretanu, I.; Ebeling, D.; Andersson, M. P.; Stipp, S. L. S.; Philipse, A.; Stuart, M. C.; van den Ende, D.; Mugele, F. Direct Observation of Ionic Structure at Solid-Liquid Interfaces: A Deep Look Into the Stern Layer. *Sci. Rep.* **2014**, *4*, 4956.
(56) Holysz, L.; Chibowski, E. Surface Free-Energy Components of α-Alumina From Thin Layer Wicking. *Langmuir* **1992**, *8*, 717−721.
(57) Argyris, D.; Ho, T.; Cole, D. R.; Striolo, A. Molecular Dynamics Studies of Interfacial Water at the Alumina Surface. *J. Phys. Chem. C* **2011**, *115*, 2038−2046.
(58) Wang, H. F.; Velarde, L.; Gan, W.; Fu, L. Quantitative Sum-Frequency Generation Vibrational Spectroscopy of Molecular Surfaces and Interfaces: Lineshape, Polarization, and Orientation. In *Annual Review of Physical Chemistry, Vol 66*; Johnson, M. A., Martinez, T. J., Eds.; Annual Reviews, 2015; Vol. *66*; pp 189−216.
(59) Darlington, A. M.; Jarisz, T. A.; DeWalt-Kerian, E. L.; Roy, S.; Kim, S.; Azam, M. S.; Hore, D. K.; Gibbs, J. M. Separating the pH-Dependent Behavior of Water in the Stern and Diffuse Layers with Varying Salt Concentration. *J. Phys. Chem. C* **2017**, *121*, 20229−20241.
(60) Ghosh, A.; Smits, M.; Sovago, M.; Bredenbeck, J.; Müller, M.; Bonn, M. Ultrafast Vibrational Dynamics of Interfacial Water. *Chem. Phys.* **2009**, *350*, 23.
(61) Eftekhari-Bafrooei, A.; Borguet, E. Effect of Surface Charge on the Vibrational Dynamics of Interfacial Water. *J. Am. Chem. Soc.* **2009**, *131*, 12034.
(62) McGuire, J. A.; Shen, Y. R. Ultrafast Vibrational Dynamics at Water Interfaces. *Science* **2006**, *313*, 1945−1948.
(63) Bonn, M.; Bakker, H. J.; Ghosh, A.; Yamamoto, S.; Sovago, M.; Campen, R. K. Structural Inhomogeneity of Interfacial Water at Lipid Monolayers Revealed by Surface-Specific Vibrational Pump-Probe Spectroscopy. *J. Am. Chem. Soc.* **2010**, *132*, 14971−14978.
(64) Towle, S. N.; Bargar, J. R.; Brown, G. E.; Parks, G. A. Sorption of Co(II) on Metal Oxide Surfaces. *J. Colloid Interface Sci.* **1999**, *217*, 312−321.
(65) Cook, R. F.; Schrott, A. G. Calcium Segregation to Grain-Boundaries in Alumina. *J. Am. Ceram. Soc.* **1988**, *71*, 50−58.
(66) Sylwester, E. R.; Hudson, E. A.; Allen, P. G. The Structure of Uranium (VI) Sorption Complexes on Silica, Alumina, and Montmorillonite. *Geochim. Cosmochim. Acta* **2000**, *64*, 2431−2438.
(67) Scheidegger, A. M.; Lamble, G. M.; Sparks, D. L. Spectroscopic Evidence for the Formation of Mixed-Cation Hydroxide Phases upon Metal Sorption on Clays and Aluminum Oxides. *J. Colloid Interface Sci.* **1997**, *186*, 118−128.
(68) Parker, S. P. *Mcgraw-Hill Dictionary of Chemistry*; McGraw-Hill Book Company: New York City, NY, 1984; Vol. *24*, pp 232−233.

DOI: 10.1021/acs.jpcc.9b01618
J. Phys. Chem. C 2019, 123, 18315−18324